Centrality, rapidity, and transverse-momentum dependence of cold nuclear matter effects on J/ψ production in dAu, CuCu, and AuAu collisions at $\sqrt{s_{NN}} = 200$ GeV

E. G. Ferreiro,[1] F. Fleuret,[2] J. P. Lansberg,[3,4,*] and A. Rakotozafindrabe[5]

[1]*Departamento de Física de Partículas, Universidade de Santiago de Compostela, E-15782 Santiago de Compostela, Spain*
[2]*Laboratoire Leprince Ringuet, École polytechnique, CNRS/IN2P3, F-91128 Palaiseau, France*
[3]*Centre de Physique Théorique, École polytechnique, CNRS, F-91128 Palaiseau, France*
[4]*SLAC National Accelerator Laboratory, Theoretical Physics, Stanford University, Menlo Park, California 94025, USA*
[5]*IRFU/SPhN, CEA Saclay, F-91191 Gif-sur-Yvette Cedex, France*

(Received 17 March 2010; published 30 June 2010)

We have carried out a wide study of cold nuclear matter (CNM) effects on J/ψ production in dAu , CuCu and AuAu collisions at $\sqrt{s_{NN}} = 200$ GeV. We have studied the effects of three different gluon-shadowing parametrizations, using the usual simplified kinematics for which the momentum of the gluon recoiling against the J/ψ is neglected as well as an exact kinematics for a $2 \to 2$ process; namely $g + g \to J/\psi + g$ as expected from LO pQCD. We have shown that the rapidity distribution of the nuclear modification factor $R_{d\mathrm{Au}}$, and particularly its antishadowing peak, is systematically shifted toward larger rapidities in the $2 \to 2$ kinematics, irrespective of which shadowing parametrization is used. In turn, we have noted differences in the effective final-state nuclear absorption needed to fit the PHENIX dAu data. Taking advantage of our implementation of $2 \to 2$ kinematics, we have also computed the transverse momentum dependence of the nuclear modification factor, which cannot be predicted with the usual simplified kinematics. All the corresponding observables have been computed for CuCu and AuAu collisions and compared to the PHENIX and STAR data. Finally, we have extracted the effective nuclear absorption from the recent measurements of R_{CP} in dAu collisions by the PHENIX collaboration.

DOI: 10.1103/PhysRevC.81.064911 PACS number(s): 13.85.Ni, 14.40.Pq, 21.65.Jk, 25.75.Dw

I. INTRODUCTION

The J/ψ particle is considered to be one of the most interesting probes of the transition from hadronic matter to a deconfined state of QCD matter; the so-called quark-gluon plasma (QGP). In the presence of a QGP, binding of $c\bar{c}$ pairs into J/ψ mesons is predicted to be hindered due to color screening, leading to J/ψ suppression in heavy ion collisions [1].

The results of J/ψ production in AuAu collisions at $\sqrt{s_{NN}} = 200$ GeV [2] show a significant suppression. Nevertheless, PHENIX data on dAu collisions [3] have also shown a nontrivial behavior, pointing out that cold-nuclear-matter (CNM) effects play an essential role at these energies (for recent reviews see Refs. [4–6] and, for perspectives for the LHC, see Ref. [7]).

All this reveals that the interpretation of the results obtained in nucleus-nucleus collisions relies on a good understanding and a proper subtraction of the CNM effects, known to impact the J/ψ production in deuteron-nucleus collisions, where the deconfinement cannot be reached.

In previous studies [8,9], we have shown that the impact of gluon shadowing on J/ψ production depends on the partonic process producing the $c\bar{c}$ and then the J/ψ. Indeed, the evaluation of the shadowing corrections in which one treats the production as a $2 \to 2$ process ($g + g \to J/\psi + g$) shows visible differences in the nuclear modification factors when compared to the results obtained for a $2 \to 1$ process.

The former partonic production mechanism seems to be favored by the recent studies based on the color-singlet model (CSM), including [10] or not [11] s-channel-cut contributions. This also seems to be confirmed by the recent studies of higher-order QCD corrections, which have shown, on the one hand, that the problematic P_{T} dependence of the LO CSM [12] is cured when going at α_S^4 and α_S^5 [13–17] and, on the other hand, that the CSM yield at next-to-leading order (NLO) in $e^+e^- \to J/\psi + X_{\mathrm{non}\ c\bar{c}}$ [18,19] saturates the experimental values by the Belle Collaboration [20]. This does not allow for a significant color-octet (CO) component [21], which happens to be precisely the one appearing in the low-P_{T} description of hadroproduction via a $2 \to 1$ process [22]. To summarize, one is entitled to consider that the former $2 \to 2$ kinematics is the most appropriate to account for the PHENIX data.

The structure of this article is as follows. In Sec. II, we describe our approach; namely the partonic process, the shadowing parametrizations, and the implementation of the nuclear absorption that we have chosen. In Sec. III, we present and discuss our results for $R_{d\mathrm{Au}}$ versus rapidity, centrality, and transverse momentum. We particularly discuss the impact of the partonic process kinematics. Section IV is devoted to the results in AuAu and CuCu collisions. In Sec. V, we present and discuss our extraction of the effective J/ψ absorption cross section from the PHENIX dAu data, following which we conclude.

II. OUR APPROACH

To describe the J/ψ production in nucleus collisions, our Monte Carlo framework [8,9] is based on the probabilistic Glauber model, the nuclear density profiles being defined with the Woods-Saxon parametrization for any nucleus $A > 2$ and

*Present address at Ecole Polytechnique.

the Hulthen wave function for the deuteron [23]. The nucleon-nucleon inelastic cross section at $\sqrt{s_{NN}} = 200$ GeV is taken to $\sigma_{NN} = 42$ mb and the maximum nucleon density to $\rho_0 = 0.17$ nucleons/fm^3.

A. Partonic process for $c\bar{c}$ production

Most studies of CNM effects on J/ψ production [24] rely on the assumption that the $c\bar{c}$ pair is produced by a $2 \to 1$ partonic process where both initial particles are gluons carrying some intrinsic transverse momentum k_T. The sum of the gluon intrinsic transverse momentum is transferred to the $c\bar{c}$ pair, thus to the J/ψ since the soft hadronization process does not significantly modify the kinematics. This is supported by the picture of the color evaporation model (CEM) at LO (see Ref. [25] and references therein) or of the CO mechanism at α_S^2 [22]. In such approaches, the transverse momentum P_T of the J/ψ is meant to come entirely from the intrinsic transverse momentum of the initial gluons.

As just discussed, recent CSM-based studies [10,11] have shown agreement with the PHENIX pp data [26] and the problematic P_T dependence of the LO CSM has been shown to be cured at Tevatron energies when going at α_S^4 and α_S^5 [13–17]. Furthermore, $e^+e^- \to J/\psi + X_{\text{non } c\bar{c}}$ NLO computations in the CSM [18,19] leave now too small a room for a CO component which would support $2 \to 1$ production kinematics [22].

Parallel to this, intrinsic transverse momentum is not sufficient to describe the P_T spectrum of quarkonia produced in hadron collisions [25]. For P_T above approximately 2–3 GeV, one expects that most of the transverse momentum should have an extrinsic origin, that is, the J/ψ's P_T would be balanced by the emission of a recoiling particle in the final state. The J/ψ would then be produced by gluon fusion in a $2 \to 2$ process with emission of a hard final-state gluon. This emission has a definite influence on the kinematics of J/ψ production. Indeed, for a given J/ψ momentum (thus for fixed y and P_T), the process $g + g \to J/\psi + g$ will proceed, on average, from gluons with larger Bjorken-x than $g + g \to c\bar{c} \to J/\psi(+X)$. Therefore, they will be affected by different shadowing corrections. From now on, we will refer to the latter $2 \to 1$ scenario as the intrinsic scheme and to the former $2 \to 2$ as the extrinsic scheme.

In the intrinsic scheme, we use the fits to the rapidity y and P_T spectra measured by PHENIX [26] in pp collisions at $\sqrt{s_{NN}} = 200$ GeV as inputs of the Monte Carlo code. The measurement of the J/ψ momentum completely fixes the longitudinal momentum fraction carried by the initial partons:

$$x_{1,2} = \frac{m_T}{\sqrt{s_{NN}}} \exp(\pm y) \equiv x_{1,2}^0(y, P_T), \tag{1}$$

with the transverse mass $m_T = (M^2 + P_T^2)^{1/2}$, with M being the J/ψ mass.

On the other hand, in the extrinsic scheme, information from the data alone—the y and P_T spectra—is not sufficient to determine x_1 and x_2. Indeed, the presence of a final-state particle introduces further degrees of freedom in the kinematics, allowing more than one value of (x_1, x_2) for a given set (y, P_T)—which are ultimately the measured quantities as opposed to (x_1, x_2). The quadri-momentum conservation explicitly results in a more complex expression of x_2 as a function of (x_1, y, P_T):

$$x_2 = \frac{x_1 m_T \sqrt{s_{NN}} e^{-y} - M^2}{\sqrt{s_{NN}}(\sqrt{s_{NN}} x_1 - m_T e^{y})}. \tag{2}$$

Equivalently, a similar expression can be written for x_1 as a function of (x_2, y, P_T). In this case, models are mandatory to compute the proper weighting of each kinematically allowed (x_1, x_2). This weight is simply the differential cross section at the partonic level times the gluon parton distribution functions (PDFs); that is, $g(x_1, \mu_f) g(x_2, \mu_f) d\sigma_{gg \to J/\psi + g}/(dy dP_T dx_1 dx_2)$. In the present implementation of our code, we are able to use the partonic differential cross section computed from any theoretical approach. For now, we use the one from Ref. [10], which takes into account the s-channel-cut contributions [27] to the basic CSM and satisfactorily describes the data down to very low P_T. A study using other matrix elements (LO CSM, NLO CEM, ...) is planned for future works.

B. Shadowing

To get the J/ψ yield in pA and AA collisions, a shadowing-correction factor has to be applied to the J/ψ yield obtained from the simple superposition of the equivalent number of pp collisions. This shadowing factor can be expressed in terms of the ratios R_i^A of the nuclear parton distribution functions (nPDF) in a nucleon of a nucleus A to the PDF in the free nucleon.

These parametrizations provide the nuclear ratios R_i^A of the PDFs:

$$R_i^A(x, Q^2) = \frac{f_i^A(x, Q^2)}{A f_i^{\text{nucleon}}(x, Q^2)}, \quad i = q, \bar{q}, g. \tag{3}$$

The numerical parametrization of $R_i^A(x, Q^2)$ is given for all parton flavors. Here, we restrain our study to gluons since,

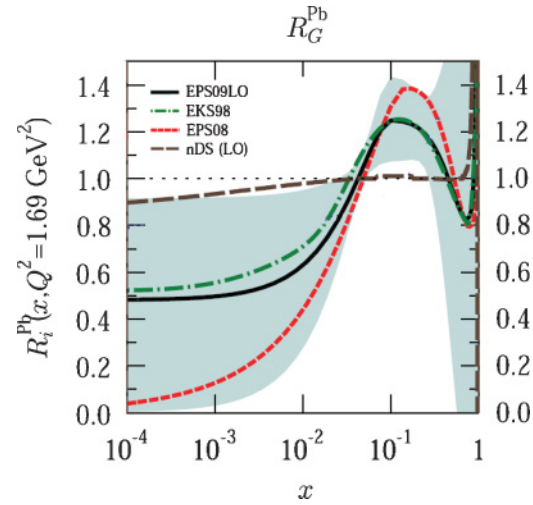

FIG. 1. (Color online) Comparison of the gluon shadowing parametrizations EKS98 [28], EPS08 [29], nDS [30] at LO, and EPS09 [31] at LO in a lead nucleus at $Q^2 = 1.69$ GeV^2. Adapted from Ref. [31].

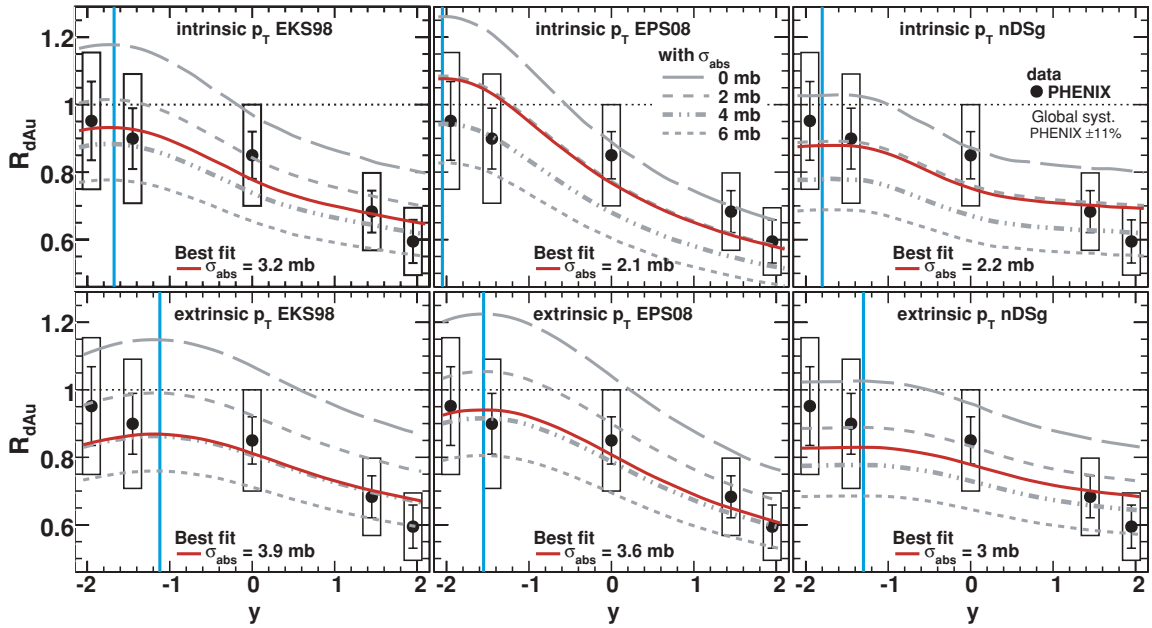

FIG. 2. (Color online) J/ψ nuclear modification factor $R_{d\mathrm{Au}}$ in dAu collisions at $\sqrt{s_{NN}} = 200$ GeV versus y in the intrinsic (top row) and extrinsic (lower row) schemes using the following gluon shadowing parametrizations: EKS98 [28] (left), EPS08 [29] (middle), and nDSg [30] (right). The vertical lines indicate qualitatively the antishadowing peak and its shifts toward larger y in the extrinsic scheme.

at high energy, J/ψ is essentially produced through gluon fusion [25].

We shall consider three different shadowing parametrizations for comparison: EKS98 [28], EPS08 [29], and nDSg [30] at LO. Recently, a new parametrization, EPS09 [31], has been made available. It offers the possibility of properly taking into account the errors arising from the fit procedure. Yet, in the case of gluon nPDF, as illustrated by Fig. 1, the region spanned by this parametrization is approximately bounded by both the nDS and EPS08 parametrizations. However, we shall not consider the nDS parametrization, which shows such small shadowing corrections that no significant yield corrections are expected. We shall prefer to use nDSg as done in other works since it provides a lower bound of EPS09 in the antishadowing region. Furthermore, the central curve of EPS09 is very close to EKS98. In this context, we have

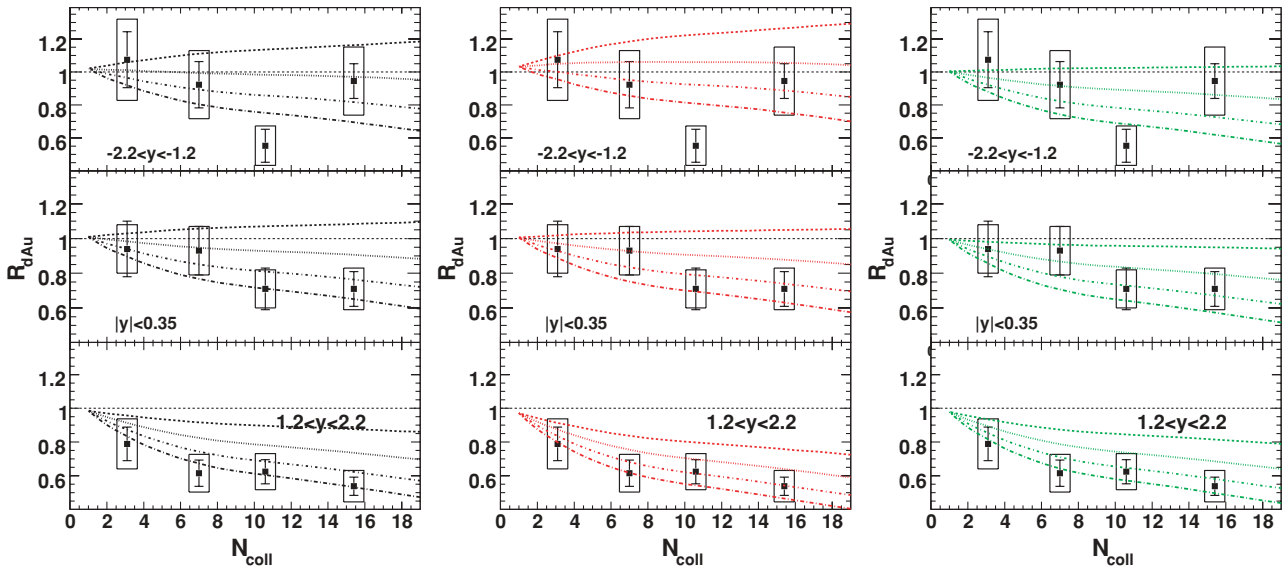

(a) EKS98 (b) EPS08 (c) nDSg

FIG. 3. (Color online) J/ψ nuclear modification factor $R_{d\mathrm{Au}}$ in dAu collisions at $\sqrt{s_{NN}} = 200$ GeV versus the number of collisions for three rapidity ranges and for four values of the nuclear absorption (from top to bottom: $\sigma_{\mathrm{abs}} = 0$, 2, 4, and 6 mb) using (a) EKS98, (b) EPS08, and (c) nDSg in the extrinsic scheme.

found it reasonable to limit our studies to EKS98, EPS08, and nDSg and to postpone to a further study the analysis of the error correlations and their impacts of J/ψ production studies.[1] Note that the spatial dependence of the shadowing has been included in our approach, assuming an inhomogeneous shadowing proportional to the local density [34,35].

[1]Note that, as shown in Fig. 1, the EPS08 parametrization shows a strong gluon shadowing at very small x due to the inclusion of forward-rapidity BRAHMS data in the fit. An explanation for such an effect has been based on the idea that, in this kinematic region that corresponds to the beam fragmentation region at large Feynman x_F, one can reach the smallest values of the momentum-fraction variable x_2 in nuclei. It makes it possible to access the strongest coherence effects, such as those associated with shadowing or alternatively the color glass condensate (CGC). Nevertheless, as it has been argued in Ref. [32], although at forward rapidities one accesses the smallest x_2 in the nuclear target, one simultaneously gets into the region of large x_1 of the projectile nucleon, where energy conservation becomes an issue. Indeed, as stated in Ref. [33], at large x_F (or x_1) one expects a suppression from Sudakov form factors, giving the probability that no particle be produced as $x_F \to 1$, as demanded by energy conservation. In a pA collision, the multiple interactions of the nucleon remnants with the nucleus makes this less likely to occur, and the suppression is expected to be stronger. In fact, factorization breaks down and the effective parton distributions in the projectile nucleon then become correlated with the nucleus target (see Eq. (15) of Ref. [33]). This effect should not be confused with gluon shadowing or other manifestations of coherence. Because of this, the strength of EPS08 gluon shadowing may be overestimated, since it includes data at large x_F which were analysed assuming that the suppression was attributed only to a reduction of the gluon distribution in the nucleus. However, we would like to emphasize that, while the gluon shadowing in EPS08 and EKS98 differ by a factor 3 at $Q^2 = 1.69$ GeV^2, the difference is already less than 20% at $Q^2 \simeq M^2_{J/\psi}$ which is the relevant scale for our analysis.

C. The nuclear absorption

The second CNM effect that we have taken into account concerns the nuclear absorption. In the framework of the probabilistic Glauber model, this effect refers to the probability for the preresonant $c\bar{c}$ pair to survive the propagation through the nuclear medium and is usually parametrized by an effective absorption cross section $\sigma_{\rm abs}$. Our results will be first shown for different values of $\sigma_{\rm abs}$ by using the three aforementioned shadowing parametrizations. Next, we will extract the values that provide the best fit to the PHENIX data. We note here that this effective cross section may also account for initial-state effects, such as parton energy loss in the nuclear target.

III. RESULTS FOR dAu COLLISIONS

The J/ψ suppression is usually characterised by the nuclear modification factor R_{AB}; that is, the ratio obtained by normalising the J/ψ yield in ion collisions to the J/ψ yield in proton collisions at the same energy times the average number of binary inelastic nucleon-nucleon collisions $N_{\rm coll}$:

$$R_{AB} = \frac{dN^{J/\psi}_{AB}}{\langle N_{\rm coll}\rangle dN^{J/\psi}_{pp}}. \tag{4}$$

Any nuclear effect affecting J/ψ production leads to a deviation of R_{AB} from unity.

A. $R_{d\rm Au}$ vs rapidity: distribution shift

In Fig. 2, we show $R_{d\rm Au}$ versus y according to both the extrinsic and intrinsic schemes. The results are displayed for four values of $\sigma_{\rm abs}$ for each of the aforementioned shadowing

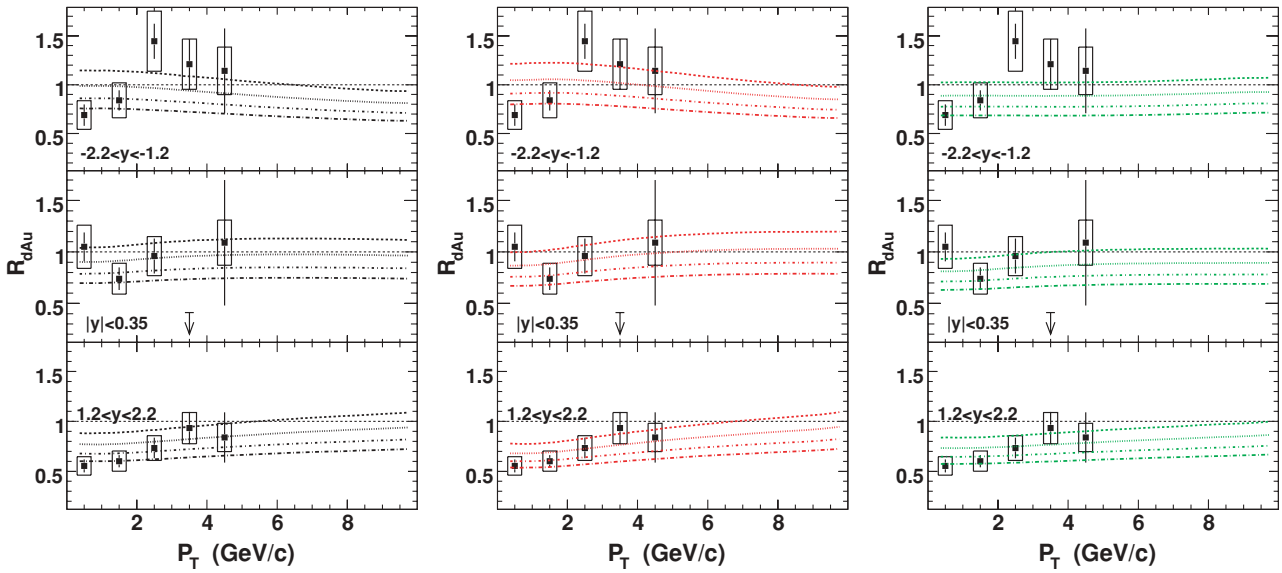

(a) EKS98 (b) EPS08 (c) nDSg

FIG. 4. (Color online) J/ψ nuclear modification factor $R_{d\rm Au}$ in dAu collisions at $\sqrt{s_{NN}} = 200$ GeV versus the transverse momentum for three rapidity ranges and for four values of the nuclear absorption (from top to bottom: $\sigma_{\rm abs} = 0$, 2, 4, and 6 mb) using (a) EKS98, (b) EPS08, and (c) nDSg in the extrinsic scheme.

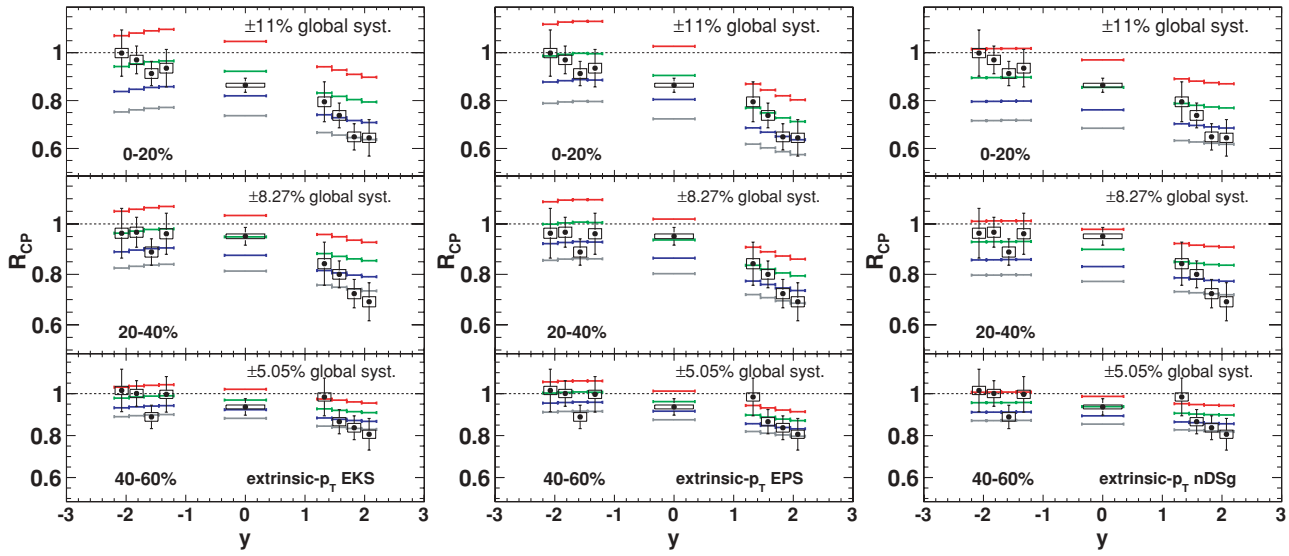

(a) EKS98 (b) EPS08 (c) nDSg

FIG. 5. (Color online) J/ψ central to peripheral nuclear modification factor $R_{\rm CP}$ in dAu collisions, at $\sqrt{s_{NN}} = 200$ GeV versus rapidity for three centrality ranges and four values of nuclear absorption (from top to bottom: $\sigma_{\rm abs} = 0$, 2, 4, and 6 mb) using (a) EKS98, (b) EPS08, and (c) nDSg.

parametrizations and are compared with the PHENIX data [3]. The best fit result as performed in Sec. V is also shown.

The comparison between the three plots on the upper row and their corresponding plots on the lower row shows a striking—but expectable—feature: The rapidity distribution in the extrinsic scheme is systematically shifted toward larger y compared to the intrinsic case. This is particularly visible when one focuses on the antishadowing peak, which we have indicated qualitatively with vertical lines.

Such a shift is, in fact, not surprising at all. It simply reflects the larger value of the gluon momentum fraction x_2 in the nucleus needed to produce a J/ψ when the momentum of the final state gluon is explicitly taken into account in the computations.

As mentioned above, recent theoretical studies of J/ψ production in vacuum (i.e., in pp collisions), support at low and mid $P_{\rm T}$ a partonic production mechanism as given by LO pQCD, namely $gg \to J/\psi g$, as opposed to a $2 \to 1$ process. In this context, we claim that this rapidity shift—evident for any shadowing parametrization—is a feature of J/ψ production in dAu that should be systematically accounted for. Along the same line of reasoning, we shall focus in the following discussions on the results obtained in the extrinsic scheme ($2 \to 2$ case), except for the extraction of $\sigma_{\rm abs}$ using the $R_{d\rm Au}$ and $R_{\rm CP}$ results.

B. $R_{d\rm Au}$ versus centrality

In Fig. 3, we present our results for $R_{d\rm Au}$ versus centrality, expressed as the number of collisions. We have taken into account the three shadowing parametrizations and four values of $\sigma_{\rm abs}$. One observes the effect of the impact-parameter dependence of the shadowing—increasing for inner production

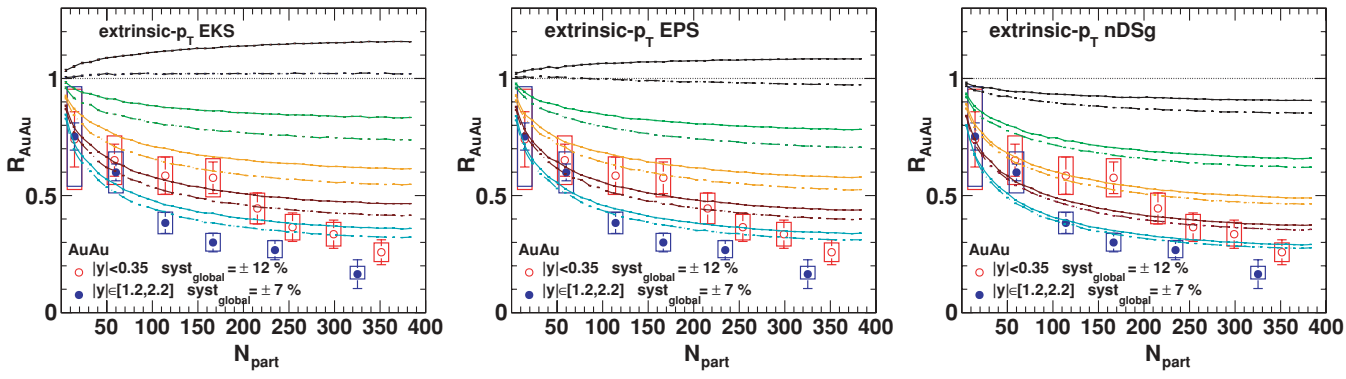

(a) EKS98 (b) EPS98 (c) nDSg

FIG. 6. (Color online) Centrality dependence of $R^{\rm mid}_{\rm AuAu}$ (solid lines) and $R^{\rm forward}_{\rm AuAu}$ (dashed lines) for five values of the nuclear absorption (from top to bottom: $\sigma_{\rm abs} = 0$, 2, 4, 6, and 8 mb) using (a) EKS98, (b) EPS08, and (c) nDSg, compared with the corresponding PHENIX data [2].

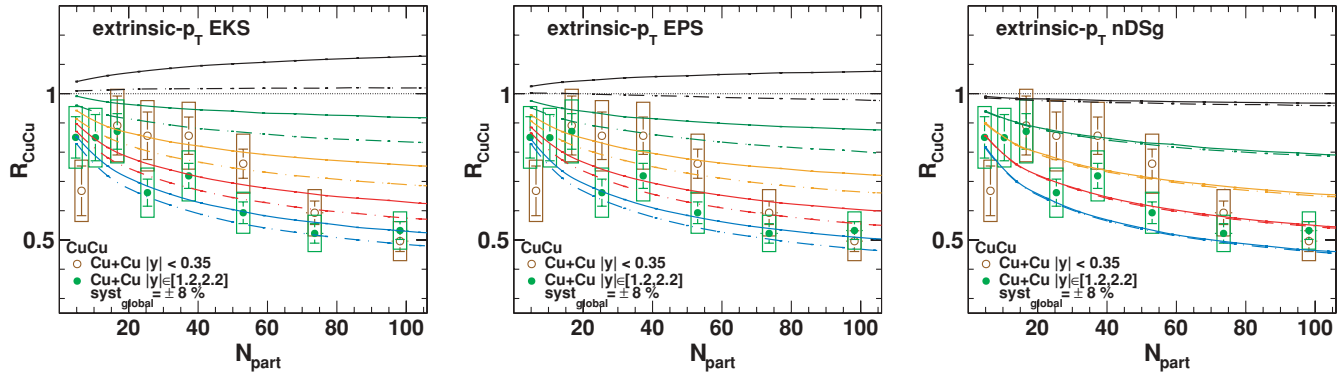

(a) EKS98 (b) EPS98 (c) nDSg

FIG. 7. (Color online) centrality dependence of $R^{\rm mid}_{\rm CuCu}$ (solid lines) and $R^{\rm forward}_{\rm CuCu}$ (dashed lines) for five values of the nuclear absorption (from top to bottom: $\sigma_{\rm abs} = 0$, 2, 4, 6, and 8 mb) using (a) EKS98, (b) EPS08, and (c) nDSg, compared with the corresponding PHENIX data [2].

points—which induces a progressive increase (decrease) versus $N_{\rm coll}$ in the backward (forward) due to the antishadowing (shadowing) effect. Indeed, for collisions with larger $N_{\rm coll}$, the J/ψ creation points are, on average, closer to the gold nucleus center where the shadowing is expected to be stronger. For the same reason, the absorption suppresses the yield more strongly for larger $N_{\rm coll}$.

The overall effect (see Fig. 3) matches the trend of the PHENIX data [3], showing a decrease versus $N_{\rm coll}$ that is stronger in the forward region than in the backward region.

We also note that the STAR collaboration has recently released a preliminary measurement of $R_{d\rm Au}$ in the region $|y| < 0.5$ using the most central collisions 0%–20% [36]: $R_{d\rm Au} = 1.45 \pm 0.60$. However, higher statistics are needed to draw conclusions from those data.

C. $R_{d\rm Au}$ versus transverse momentum

It is important to note that, in order to predict the transverse momentum dependence of the shadowing corrections, one needs to resort to a model which contains an explicit dependence on $P_{\rm T}$. Studies were earlier carried on using the CEM at NLO in [37]. However, due to the complexity inherent to the NLO code used, it was not possible to implement the impact-parameter dependence of the shadowing needed to reproduce, for instance, the centrality dependence [34,35] as just discussed. Thanks to the versatility of our Glauber code, we can carry on such computations including such an impact-parameter dependence as well as involved production mechanisms containing a nontrivial dependence on $P_{\rm T}$.

In Fig. 4, we show our results on $R_{d\rm Au}$ versus the transverse momentum. We emphasise that the growth of $R_{d\rm Au}$ is not related to any Cronin effect, since it is not taken into account here. It simply comes from the increase of x_2 for increasing $P_{\rm T}$ as given by Eq. (2). Hence, in the mid- and forward-rapidity region, x_2 goes through the antishadowing region and one observes an enhancement in $R_{d\rm Au}$. In the backward region, where x_2 sits in an antishadowing region, one only sees a decrease. A similar behavior is obviously expected in R_{AA} versus $P_{\rm T}$ as will be discussed in Sec. IV C.

D. $R_{\rm CP}$

New results for the J/ψ from the 2008 dAu run with approximately thirty times larger integrated luminosity than the 2003 dAu results are emerging, with the first preliminary result in terms of $R_{\rm CP}$ [38],

$$R_{\rm CP} = \frac{\left(\frac{dN_{J/\psi}}{dy} \Big/ N_{\rm coll}\right)}{\left(\frac{dN^{60-80\%}_{J/\psi}}{dy} \Big/ N^{60-80\%}_{\rm coll}\right)}. \quad (5)$$

Those recent data show a significant dependence on the rapidity, with a visible suppression for the most forward points in the three centrality ranges (0%–20%, 20%–40%, and 40%–60%). In the negative rapidity region, which is

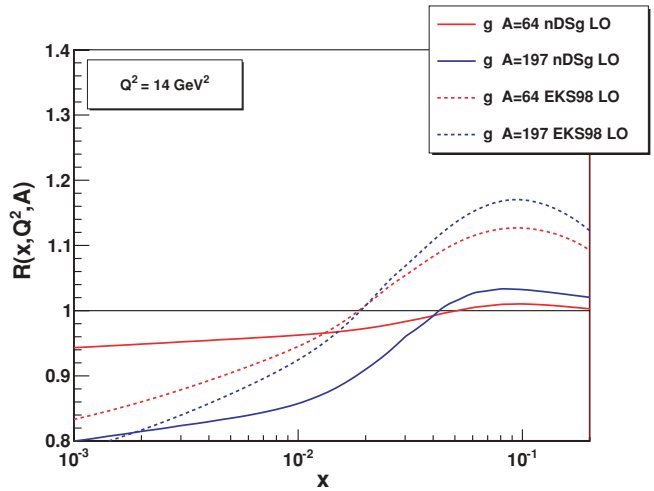

[a]The plot has been generated by the nPDF generator http://lappweb.in2p3.fr/lapth/npdfgenerator.

FIG. 8. (Color online) Comparison of the gluon shadowing parametrizations EKS98 [28] and nDSg [30] in lead and copper nuclei at $Q^2 = 14$ GeV^2.[a]

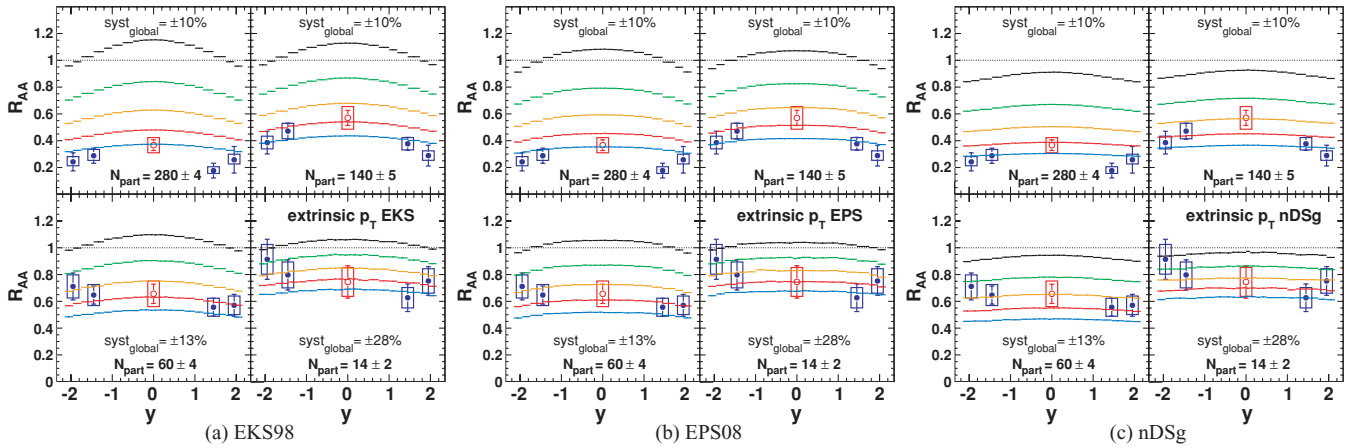

(a) EKS98 (b) EPS08 (c) nDSg

FIG. 9. (Color online) R_{AA} versus y for AuAu collisions for five values of $\sigma_{\rm abs}$ (from top to bottom: $\sigma_{\rm abs} = 0$, 2, 4, 6, and 8 mb) using (a) EKS98, (b) EPS08, (c) nDSg in 4 centrality bins.

expected to be dominated by large x_2 contributions,[2] the data (see Fig. 5) show approximately no nuclear effects within the uncertainties, but a visible suppression is observed at mid and forward rapidities. We also note that the suppression is stronger in most central collisions. As regards our results, Fig. 5 shows the rapidity dependence of the modification factor $R_{\rm CP}$ for the three centrality ranges using the EKS98, EPS08, and nDSg shadowing parametrizations. Different break-up cross sections have also been considered, from 0 to 6 mb. As announced, we have chosen to focus on the extrinsic scheme. Like for $R_{d\rm Au}$, this induces differences on the shadowing impact compared to the intrinsic scheme used in Ref. [39]. One observes in Fig. 5 that the trend of the data is reasonably described with a $\sigma_{\rm abs}$ in the range of 2–4 mb, while the most forward points seem to decrease more than our evaluation. However, the uncertainties affecting the present preliminary measurements precludes drawing firmer conclusions. We shall analyze this in more detail in Sec. V.

[2]One recalls here that in the extrinsic scheme there is no one-to-one mapping between the rapidity and the momentum fraction of the initial gluon, and yet they are correlated.

IV. RESULTS FOR CuCu AND AuAu COLLISIONS

A. Centrality dependence[3]

In Figs. 6 and 7, we present the centrality dependence of the nuclear modification factor $R_{\rm AuAu}$ and $R_{\rm CuCu}$ in the forward and mid rapidity regions. This has been computed for the three shadowing parametrizations and for five values of $\sigma_{\rm abs}$.

As we have already observed in Ref. [9], R_{AA} is systematically smaller in the forward region than in the mid-rapidity region (see also the next section). The difference increases for more central collisions since we have used an impact parameter dependent shadowing. While this difference (approximatively 20% for rather central collisions) matches well the one of the data when $\sigma_{\rm abs} = 0$, one would have to choose a large $\sigma_{\rm abs}$ if one wanted to reproduce the normalisation of the AuAu data, disregarding any effects of hot nuclear matter (HNM). However, for such large $\sigma_{\rm abs}$, surviving J/ψ from inner production points would be so rare that the difference between shadowing effects at mid and forward rapidities would

[3]As announced, we focus on the extrinsic case in all the following discussions.

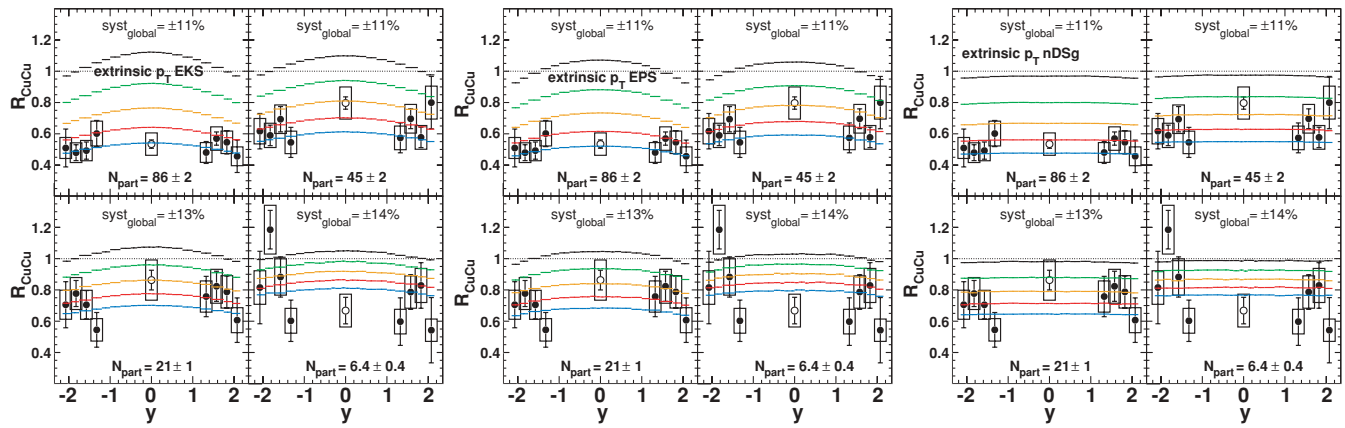

(a) EKS98 (b) EPS08 (c) nDSg

FIG. 10. (Color online) R_{AA} versus y for CuCu collisions for five values of $\sigma_{\rm abs}$ (from top to bottom: $\sigma_{\rm abs} = 0$, 2, 4, 6, and 8 mb) using (a) EKS98, (b) EPS08, and (c) nDSg in 4 centrality bins.

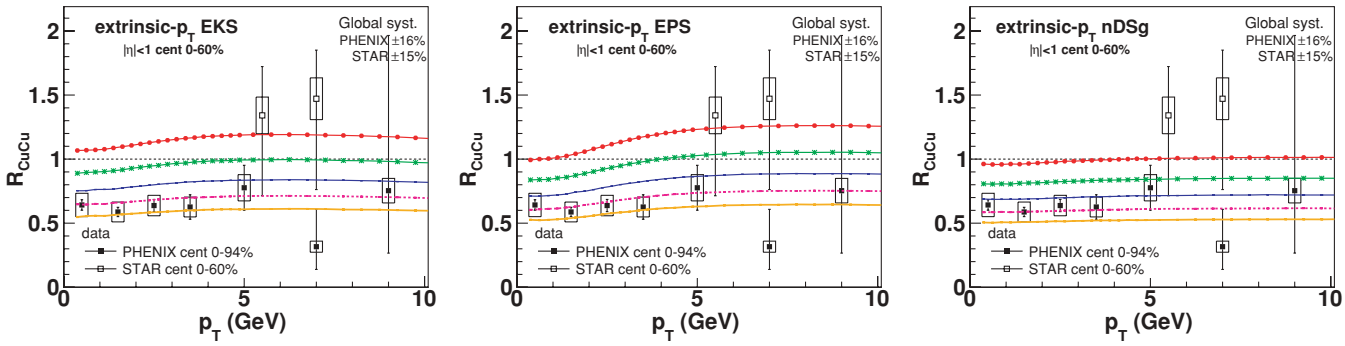

(a) EKS98 (b) EPS08 (c) nDSg

FIG. 11. (Color online) J/ψ nuclear modification factor in CuCu collisions at $\sqrt{s_{NN}} = 200$ GeV versus P_{T} for the mid-rapidity region for five values of the nuclear absorption (from top to bottom: $\sigma_{\mathrm{abs}} = 0$, 2, 4, 6, and 8 mb) using (a) EKS98, (b) EPS08, and (c) nDSg. Those are compared with the two STAR points [41] and the PHENIX preliminary results [42].

nearly vanish. Note that for a σ_{abs} in the range of 2–4 mb, a difference remains.

While most of the above discussion is similar for CuCu collisions using the EKS and EPS shadowing, one observes a peculiar feature for nDSg. Indeed, one does not observe any effect. This comes for the very weak shadowing encoded in nDSg for Cu. This is illustrated in Fig. 8, where one sees that nDSg shadowing in Cu nucleus ends up to be very small. Indeed, while there is a moderate difference between the EKS shadowing in Cu and in Au, there is a significant difference for nDSg.

B. Rapidity dependence

We now discuss the rapidity dependence of the nuclear modification factor in the case of CuCu and AuAu collisions. It is displayed in Figs. 9 and 10 for the three shadowing parametrizations and for five values of σ_{abs}. As in Ref. [9], R_{AA} slightly peaks at $y = 0$, reducing the need for recombination effects [40] which are particularly concentrated in the mid rapidity region and which could elegantly explain the differences of R_{AA} between the forward- and mid-rapidity regions.

As we have noted in the previous section, shadowing effects exhibit naturally such a rapidity dependence. This happens for the three shadowing parametrizations we have used for AuAu, confirming that this is a feature, rather than an accident. This effect is, however, reduced when an absorption cross section is accounted for. It is widely accepted that HNM effects are responsible for an extra suppression. If this suppression—by the creation of a QGP for instance—is not correlated to the path of the $c\bar{c}$ on its way out of the nuclei, it may not damp down the difference between $R_{AA}^{\mathrm{forward}}$ and R_{AA}^{mid}, as does a larger σ_{abs}.

C. Transverse-momentum dependence

We now move on to the discussion of the transverse momentum dependence in the mid-rapidity region, analyzed both by the PHENIX [42] and STAR [41] collaborations. As announced during the discussion of the dAu results, R_{AA} versus P_{T} increases with P_{T} (see Fig. 11). In fact, the growth partially matches the trend of the PHENIX and STAR data. We should, however, mention here that there is no consensus for now on whether one should expect a nuclear modification factor larger than one for P_{T} around 8 GeV as seems to indicate the published STAR results [41].

In the case of a confirmation of a nonsuppression of J/ψ at large P_{T}, one could say that it does not behave as the other

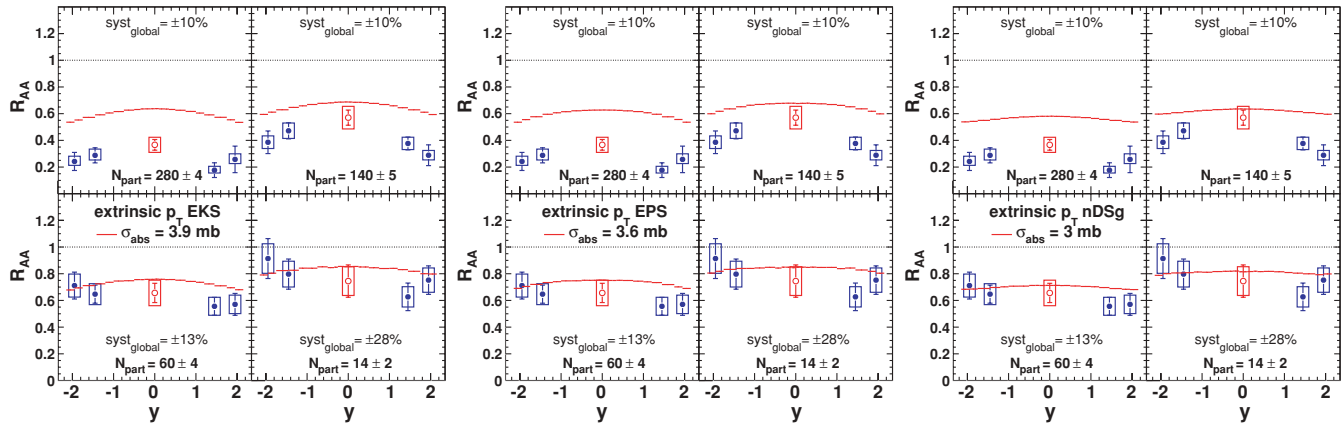

(a) EKS98 (b) EPS08 (c) nDSg

FIG. 12. (Color online) R_{AA} versus y for AuAu collisions for the best σ_{abs} as obtained from the fit to the dAu data using (a) EKS98, (b) EPS08, and (c) nDSg in 4 centrality bins.

TABLE I. $\sigma_{\rm abs}$ extracted from fit of $R_{d\rm Au}$ (all cross section in unit of mb).

	$\sigma_{\rm abs}$	$\chi^2_{\rm min}$
EKS98 Int.	3.2 ± 2.4	0.9
EPS08 Int.	$2.1^{+2.6}_{-2.2}$	1.1
nDSg Int.	$2.2^{+2.3}_{-2.1}$	1.3
EKS98 Ext.	$3.9^{+2.7}_{-2.3}$	1.1
EPS08 Ext.	$3.6^{+2.4}_{-2.5}$	0.5
nDSg Ext.	$3.0^{+2.2}_{-2.4}$	1.2

TABLE II. $\sigma_{\rm abs}$ and their errors[a] extracted from fit of the $R_{\rm CP}$ data averaged on three rapidity regions as well as on the entire range (all cross sections in units of mb).

	$y < 0$	$y = 0$	$y > 0$	All y
EKS98 Int. [39]	5.2 ± 1.2	3.1 ± 1.3	9.5 ± 1.4	N/A
EKS98 Ext.	2.5 ± 0.5	3.2 ± 0.5	4.8 ± 0.7	3.2 ± 0.4
EPS08 Ext.	3.2 ± 0.5	2.5 ± 0.5	3.1 ± 0.6	2.9 ± 0.3
nDSg Ext.	1.4 ± 0.5	1.6 ± 0.5	4.0 ± 0.7	2.2 ± 0.3

[a]The errors quoted for the first line are extracted differently than ours. The errors shown here should only be compared for a given analysis.

hadrons, which are significantly suppressed in central Cu+Cu collisions and for increasing $P_{\rm T}$ (see Ref. [43] for π^0 and Ref. [44] for "heavy-flavor" muons). In fact, the J/ψ seems to adopt a behavior closer to the one of prompt photons [45] than to the one of other (heavy-flavored) hadrons. We also note a nonsuppression of ϕ meson in central Cu + Cu collisions [46].

If one goes further, one may want to extract information about the production mechanism at work here. Indeed, although the energy loss of a colored object in CNM is limited to be constant, rather than scaling with energy, by the Landau-Pomeranchuk-Migdal effect [47], its magnitude per unit length will be significantly larger for a CO than for a CS state propagating in the nuclear matter. This is especially relevant since, in the mid-rapidity region, the $c\bar{c}$ pair hadronizes outside the nucleus. This would naturally lead us to the conclusion that it is rather a colorless state than a colored one which propagates in the nuclear matter.

V. EXTRACTION OF BREAK-UP CROSS SECTION BY FITS OF *d*Au DATA

By comparing our results in the intrinsic and extrinsic approaches, we have learned that one of the consequences of this kinematical change implies a shift of the rapidity distribution. The latter is shifted as a whole to larger values of rapidity in the extrinsic case. As usual, a J/ψ break-up cross section $\sigma_{\rm abs}$ has to be accounted for to describe the normalization of $R_{d\rm Au}$. In practice, it is fit from the data and then used in the description of nucleus-nucleus collisions. In view of the differences of the shadowing impact induced by one or the other kinematics, it is natural to wonder what the corresponding variations of $\sigma_{\rm abs}$ fit to the data are.

A. Fitting $R_{d\rm Au}$ data

For this purpose, we have used PHENIX measurements of $R_{d\rm Au}$ [3] in order to obtain the best fit of $\sigma_{\rm abs}$ for each of the shadowing parametrization considered in both the intrinsic and extrinsic schemes. Based on the method used by PHENIX in Refs. [3] and [48], we have computed the χ^2 in the different cases, including both statistical and systematic errors.

By using the data on $R_{d\rm Au}$ versus rapidity, we have obtained the values of $\sigma_{\rm abs}$ given in Table I for each of the shadowing parametrizations and for both production schemes. The resulting curves are shown in Fig. 2 for dAu, and in Figs. 12 and 13 for AuAu and CuCu.

In general, fitting the rapidity with a constant $\sigma_{\rm abs}$ leads to a more-than-acceptable χ^2. The largest ones are obtained for the nDSg parametrization; this confirms the impression that parametrization with "significant" shadowing or antishadowing (EKS98, EPS08) are preferred by the data (see also Fig. 2). The only systematic one can really see is that the 3 $\sigma_{\rm abs}$ values extracted using the extrinsic scheme are larger than

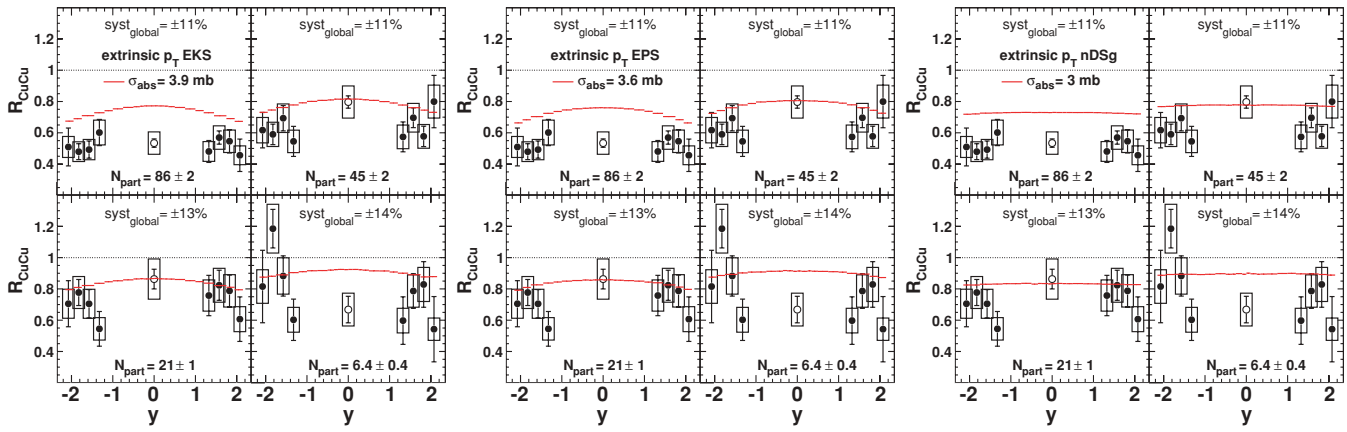

(a) EKS98 (b) EPS08 (c) nDSg

FIG. 13. (Color online) R_{AA} versus y for CuCu collisions for the best $\sigma_{\rm abs}$ as obtained from the fit to the dAu data using (a) EKS98, (b) EPS08, and (c) nDSg in 4 centrality bins.

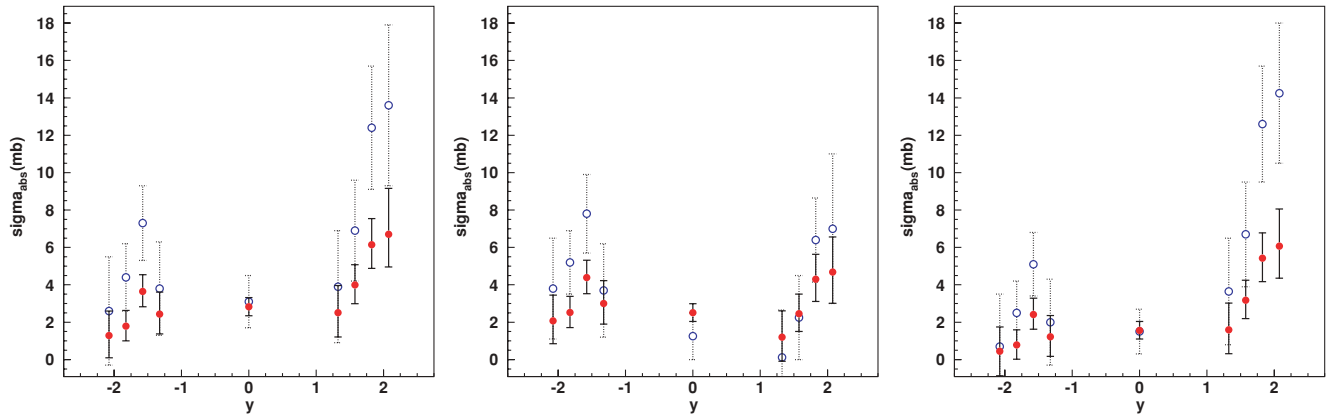

(a) EKS98 (b) EPS08 (c) nDSg

FIG. 14. (Color online) $\sigma_{\rm abs}$ versus y obtained by fitting the $R_{\rm CP}$ data for dAu, in the extrinsic scheme (in red closed circles) compared to the intrinsic scheme [39] (in blue open circles) using (a) EKS98, (b) EPS08 and (c) nDSg.

the corresponding values obtained with the intrinsic scheme, as expected due to the increase of x_2 in the extrinsic case compared to the intrinsic one. For the time being, the data are not precise enough to draw further conclusions from such fits.

B. Fitting $R_{\rm CP}$ data

We have also fit the new $R_{\rm CP}$ data with a constant $\sigma_{\rm abs}$ in each rapidity regions. Our results are given in Table II along with the one of Ref. [39] based on $2 \rightarrow 1$ kinematics and using the EKS98 shadowing. We need to make clear at this point that the intrinsic scheme used in Ref. [39] slightly differs from the one we have used, for instance, to fit the dAu data as shown in the previous section. The difference appears at the level of the running of the scale of the shadowed gluon distribution and the invariant mass of produced system. However, this is not expected to modify the following discussion (see Ref. [8]).

As can be seen in Table II, it appears that the strong suppression at forward rapidity and the lack of suppression at backward rapidity cannot be described using a fixed breakup cross section with EKS98 in the intrinsic scheme [39]. One also seems to observe an increase of $\sigma_{\rm abs}$ with rapidity in our analysis (extrinsic) for EKS98 and nDSg, but a constant behavior cannot be ruled out. The increase is in any case softer when the final-state gluon momentum is taken into account. It seems that forward rapidity is maybe the most interesting region for such investigations. Interestingly, in the case of EPS08, the value we have extracted for the forward region is equal to the one for the backward region.

As we have argued earlier, EPS08 can be used as a good indicator of the strongest shadowing reachable within the uncertainty of EPS09. From this viewpoint, the recent update of the intrinsic analysis, where [49] no increase of $\sigma_{\rm abs}$ is observed for the strongest shadowing of EPS09, confirms our findings.

To get a more precise view on the situation, it is useful to plot the effective absorptive cross section as function of the rapidity, without averaging on the three rapidity regions. The result can be seen on Fig. 14 with our result in the extrinsic scheme (red closed circles) and the one of Ref. [39] (blue open circles)[4] in the intrinsic scheme. We have obtained an increasing absorptive cross section with rapidity, but the increase is much less pronounced than in the intrinsic case. In fact, in the EPS08 case, the increase does not appear statistically significant.

VI. CONCLUSION

Taking advantage of the probabilistic Glauber Monte-Carlo framework, JIN, discussed in Refs. [8,9], we have (i) considered three different gluon shadowing parametrizations–EKS98, EPS08 and nDSg–taking into account a dependence on the impact parameter b and the momentum of the gluon recoiling against the J/ψ, (ii) shown that the rapidity dependence of $R_{d\rm Au}$ is shifted toward larger rapidities irrespective of the shadowing parametrization, and particularly the antishadowing peak, (iii) shown that the antishadowing peak is reflected in a rise of the nuclear modification factor for increasing $P_{\rm T}$, (iv) compared our results with the experimental measurements of the nuclear modification factors $R_{d\rm Au}$ and $R_{\rm CP}$ from dAu collisions presently available at RHIC and extracted the favoured values of the $c\bar{c}$ absorption cross section in the nuclear matter, and finally (v) shown that the effective absorption-cross-section increase at forward rapidity, obtained from the recent analysis of PHENIX $R_{\rm CP}$ data [39] in which the final-state gluon momentum is neglected (intrinsic case), is less marked when it is taken into account; that is, in the extrinsic case.

ACKNOWLEDGMENTS

We would like to thank S.J. Brodsky, A. Linden-Levy, C. Lourenço, N. Matagne, J. Nagle, T. Ullrich, R. Vogt,

[4]We recall here that the error bars in Fig. 14 are extracted with two different procedures in each case. They should only be compared within one approach.

H. Wöhri for stimulating and useful discussions. This work is supported in part by Xunta de Galicia (2008/012) and Ministerio de Educacion y Ciencia of Spain (FPA2008-03961-E/IN2P3), the Belgian American Educational Foundation, the Francqui Foundation and the US Department of Energy under contract number DE-AC02-76SF00515.

[1] T. Matsui and H. Satz, Phys. Lett. B **178**, 416 (1986).
[2] A. Adare *et al.*, Phys. Rev. Lett. **98**, 232301 (2007).
[3] A. Adare *et al.*, Phys. Rev. C **77**, 024912 (2008).
[4] A. D. Frawley, T. Ullrich, and R. Vogt, Phys. Rep. **462**, 125 (2008).
[5] R. Rapp, D. Blaschke, and P. Crochet, arXiv:0807.2470.
[6] L. Kluberg and H. Satz, arXiv:0901.3831.
[7] J. P. Lansberg *et al.*, AIP Conf. Proc. **1038**, 15 (2008).
[8] E. G. Ferreiro, F. Fleuret, and A. Rakotozafindrabe, Eur. Phys. J. C **61**, 859 (2009).
[9] E. G. Ferreiro, F. Fleuret, J. P. Lansberg, and A. Rakotozafindrabe, Phys. Lett. B **680**, 50 (2009).
[10] H. Haberzettl and J. P. Lansberg, Phys. Rev. Lett. **100**, 032006 (2008).
[11] S. J. Brodsky and J. P. Lansberg, Phys. Rev. D **81**, 051502(R) (2010).
[12] C.-H. Chang, Nucl. Phys. B **172**, 425 (1980); E. L. Berger and D. L. Jones, Phys. Rev. D **23**, 1521 (1981); R. Baier and R. Rückl, Phys. Lett. B **102**, 364 (1981); Z. Phys. C **19**, 251 (1983); V. G. Kartvelishvili, A. K. Likhoded, and S. R. Slabospitsky, Sov. J. Nucl. Phys. **28**, 678 (1978) [Yad. Fiz. **28**, 1315 (1978)].
[13] J. M. Campbell, F. Maltoni, and F. Tramontano, Phys. Rev. Lett. **98**, 252002 (2007).
[14] P. Artoisenet, J. P. Lansberg, and F. Maltoni, Phys. Lett. B **653**, 60 (2007).
[15] B. Gong and J. X. Wang, Phys. Rev. Lett. **100**, 232001 (2008).
[16] P. Artoisenet, J. M. Campbell, J. P. Lansberg, F. Maltoni, and F. Tramontano, Phys. Rev. Lett. **101**, 152001 (2008).
[17] J. P. Lansberg, Eur. Phys. J. C **61**, 693 (2009).
[18] B. Gong and J. X. Wang, Phys. Rev. Lett. **102**, 162003 (2009).
[19] Y. Q. Ma, Y. J. Zhang, and K. T. Chao, Phys. Rev. Lett. **102**, 162002 (2009).
[20] P. Pakhlov *et al.* (Belle Collaboration), Phys. Rev. D **79**, 071101 (2009).
[21] Y. J. Zhang, Y. Q. Ma, K. Wang, and K. T. Chao, Phys. Rev. D **81**, 034015 (2010).
[22] P. L. Cho and A. K. Leibovich, Phys. Rev. D **53**, 6203 (1996).
[23] P. E. Hodgson, *Nuclear Reactions and Nuclear Structure* (Clarendon Press, Clarendon, Oxford, 1971).
[24] T. Gousset and H. J. Pirner, Phys. Lett. B **375**, 349 (1996); R. Vogt, Phys. Rev. C **61**, 035203 (2000); F. Arleo and V. N. Tram, Eur. Phys. J. C **55**, 449 (2008); F. Arleo, Phys. Lett. B **666**, 31 (2008); C. Lourenco, R. Vogt, and H. K. Woehri, J. High Energy Phys. 02 (2009) 014.
[25] J. P. Lansberg, Int. J. Mod. Phys. A **21**, 3857 (2006).
[26] A. Adare *et al.*, Phys. Rev. Lett. **98**, 232002 (2007).
[27] J. P. Lansberg, J. R. Cudell, and Yu. L. Kalinovsky, Phys. Lett. B **633**, 301 (2006).
[28] K. J. Eskola, V. J. Kolhinen, and C. A. Salgado, Eur. Phys. J. C **9**, 61 (1999).
[29] K. J. Eskola, H. Paukkunen, and C. A. Salgado, J. High Energy Phys. 07 (2008) 102.
[30] D. de Florian and R. Sassot, Phys. Rev. D **69**, 074028 (2004).
[31] K. J. Eskola, H. Paukkunen, and C. A. Salgado, J. High Energy Phys. 04 (2009) 065.
[32] B. Z. Kopeliovich, E. Levin, I. K. Potashnikova, and I. Schmidt, Phys. Rev. C **79**, 064906 (2009).
[33] B. Z. Kopeliovich, J. Nemchik, I. K. Potashnikova, M. B. Johnson, and I. Schmidt, Phys. Rev. C **72**, 054606 (2005).
[34] S. R. Klein and R. Vogt, Phys. Rev. Lett. **91**, 142301 (2003).
[35] R. Vogt, Phys. Rev. C **71**, 054902 (2005).
[36] C. Perkins (STAR Collaboration), Nucl. Phys. A **830**, 231C (2009).
[37] M. Bedjidian *et al.*, CERN-2004-009-C.
[38] C. L. da Silva (PHENIX Collaboration), Nucl. Phys. A **830**, 227C (2009).
[39] A. D. Frawley, lecture delivered at the Joint CATHIE INT mini-program Quarkonia in Hot QCD, INT, Seattle, WA, 2009.
[40] L. Granchamp, R. Rapp, and G. E. Brown, Phys. Rev. Lett. **92**, 212301 (2004); E. L. Bratkovskaya, A. P. Kostyuk, W. Cassing, and H. Stocker, Phys. Rev. C **69**, 054903 (2004); R. L. Thews, Eur. Phys. J. C **43**, 97 (2005); L. Yan, P. Zhuang, and N. Xu, Phys. Rev. Lett. **97**, 232301 (2006); A. Andronic, P. Braun-Munzinger, K. Redlich, and J. Stachel, Nucl. Phys. A **789**, 334 (2007); A. Capella, L. Bravina, E. G. Ferreiro, A. B. Kaidalov, K. Tywoniuk, and E. Zabrodin, Eur. Phys. J. C **58**, 437 (2008).
[41] B. I. Abelev *et al.* (STAR Collaboration), Phys. Rev. C **80**, 041902 (2009).
[42] M. Leitch (PHENIX Collaboration), Nucl. Phys. A **830**, 27C (2009).
[43] A. Adare *et al.* (PHENIX Collaboration), Phys. Rev. Lett. **101**, 162301 (2008).
[44] I. Garishvili (PHENIX Collaboration), Nucl. Phys. A **830**, 625C (2009).
[45] K. Reygers (PHENIX Collaboration), J. Phys. G **35**, 104045 (2008).
[46] M. Naglis (PHENIX Collaboration), Nucl. Phys. A **830**, 757C (2009).
[47] S. J. Brodsky and P. Hoyer, Phys. Lett. B **298**, 165 (1993).
[48] A. Adare *et al.*, Phys. Rev. C **77**, 064907 (2008).
[49] A. D. Frawley, lecture delivered at the Joint CATHIE/TECHQM Workshop, BNL, Brookhaven, NY, 2009.